Contribution from the University Chemical Laboratory,
Lensfield Road, Cambridge CB2 1EW, U.K.

A Ligand-Field Probe of Transition-Metal–Oxygen Ligations

Neil D. Fenton and Malcolm Gerloch*

Received October 14, 1988

Ligand-field analyses of the electron spin resonance and optical absorption, single-crystal spectra of pentakis(picoline *N*-oxide)cobalt(II) diperchlorate and dichlorobis(triphenylphosphine oxide)cobalt(II) are reported. The ligations with the amine oxide and phosphine oxide donors are characterized by locally nondiagonal ligand fields. That for the phosphine oxide is interpreted in terms of a hybridization for the donor oxygen atom between sp^2 and sp. For the amine oxide, the ligand-field effects of "misdirected valency" arise from the formally nonbonding sp^2 oxygen lone pair. Significant differences between the local ligand fields of these picoline *N*-oxide groups and those of pyridine *N*-oxides in the complex hexakis(pyridine *N*-oxide)cobalt(II) diperchlorate are rationalized in terms of the coordination numbers in these complexes. These conclusions are underscored by Fenske–Hall molecular orbital calculations for the free picoline *N*-oxide and pyridine *N*-oxide.

Introduction

The utility of modern ligand-field analysis is owed in large measure to the exploitation of spatial superposition that establishes the separate parametrization of the ligand fields of individual ligands in locally defined σ- and π-bonding modes. In its most basic form, the cellular ligand-field (CLF) model employs the energy variables e_σ, $e_{\pi x}$, and $e_{\pi y}$ to represent d orbital energy shifts arising from each local metal–ligand interaction with effective C_{2v} *pseudo*symmetry. Where that description is unsatisfactory—and, in particular, for those ligations of local C_s symmetry—the cellular ligand field ceases to be diagonal with respect to the "natural" frame otherwise employed in most CLF studies and an extra parameter, $e_{\pi\sigma}$, is required to characterize what has been called "misdirected valency". These circumstances arise when the metal d orbitals suffer perturbation either from a misalignment of the metal–ligand bonds with respect to the line of centers—"bent bonding"—or from the presence of a formally nonbonding lone pair positioned to one side of that line and situated on the donor atoms, or to both. In a recent series of papers,[1-4] we have been able to demonstrate the ligand-field effects of both kinds of misdirected valence unequivocally. The inclusion of an $e_{\pi\sigma}$ parameter into those analyses was important, not only to demonstrate the locally nondiagonal nature of the ligand fields but also to show that values for the more usual diagonal parameters should be properly established and not take on false values in some ill-defined and averaged way.

While bent bonding, arising from ring strain in chelates or from intermolecular steric forces, for example, might be expected for all manner of ligands, the ligand-field effects of nonbonding lone pairs will be encountered most commonly, though not exclusively, for ligands with oxygen donor atoms. Similar contributions from sulfur ligators appear to be much less important in view of the longer metal–ligand bonds and more diffuse lone-pair density. Within our earlier studies, the misdirected valency probed by ligand-field analysis was clearly dominated either by lone pairs or by bent bonds separately, or their combined contributions were evident but not well disentangled. In part, the present study aims to clarify the nature of these different causes of the same effect.

We describe detailed ligand-field analyses of the single-crystal electron spin resonance $\mathbf{g}^2$ tensors and polarized electronic absorption spectra of the formally trigonal-bipyramidal complex ion pentakis(picoline *N*-oxide)cobalt(II) and of the tetrahedral molecule dichlorobis(triphenylphosphine oxide)cobalt(II). Unique sets of ligand-field parameters have been obtained for each system and provide interesting reflections of the natures of the ligations of cobalt with these amine oxide and phosphine oxide ligands. The ligand fields offered by the picoline *N*-oxides are to be contrasted with those of the pyridine *N*-oxides in the hexakis(pyridine *N*-oxide)cobalt(II) ion established earlier. Our explanation of the differences are complemented by Fenske–Hall molecular orbital calculations for these ligands. Overall, the focus of the present study is the nature of the metal–ligand bonding itself, as much as the ligand-field properties that probe it.

Analyses

All calculations have been carried out by using the CAMMAG2 computing suite[5] developed in this laboratory initially within the restricted spin-quartet basis, $^4F + {}^4P$, but finally within the 120-fold basis of the complete d^7 configuration. We describe analyses of d–d transition energies and ESR $\mathbf{g}^2$ tensors for each complex. Basis functions were expressed within J,M_J quantization throughout. Computational details and program schemes encoded in the CAMMAG2 suite have been outlined in ref 5b,c. The calculation of ESR $\mathbf{g}^2$ tensors is discussed in ref 5d,e.

Pentakis(picoline *N*-oxide)cobalt(II) Diperchlorate. Cobalt–oxygen bond lengths[6] for the axial ligations in the formal trigonal bipyramid shown in Figure 1 are 2.06 and 2.10 Å and, for the equatorial ones, 1.99, 1.99, and 1.98 Å. The angles ∠Co–O–N are 119 and 121° for the axial ligands and 124, 120, and 129° for the equatorial. Our ligand-field analysis, therefore, parametrizes the axial and equatorial ligand fields as two distinct sets with e_σ, $e_{\pi\perp}$, $e_{\pi\parallel}$, and $e_{\pi\sigma}$ variables for each. Parallel and perpendicular are defined with respect to the local planes of appropriate Co–O–N triads, and the off-diagonal parameters, $e_{\pi\sigma}$, refer to misdirected valency in those planes. In addition, we have the usual Racah *B* and *C* parameters for interelectron repulsion, and ζ for spin–orbit coupling, together with the orbital reduction factor *k* in the magnetic moment operators.

The optical spectra[6] are not rich and could not support so heavily parametrized an analysis on their own. We began, therefore, by seeking to reproduce the observed ESR $\mathbf{g}^2$ tensor.[7] This has been reported for the cobalt-doped zinc analogue in detail but confirmed from ESR studies of the pure cobalt complex. Wide variations of all parameter values have been considered throughout the analysis: in particular, e_σ has been varied between 2500 and 6000 cm^{-1} for each ligand type; e_π between −1000 and +2500 cm^{-1}; $e_{\pi\sigma}$ between ±1500 cm^{-1}.

No combination of these parameter values whatever was found to yield an even remotely acceptable reproduction of the reported $\mathbf{g}^2$ tensor. Successful reproduction *can* be achieved, however, if the experimental axes are relabeled such that $\{a'bc\} \rightarrow \{c'ba\}$. Personal communication with Professor D. Gatteschi has confirmed that a typographical error with that result had characterized the original experimental paper.[7] We are grateful for his confirmation and note meanwhile how confidence may be placed in modern ligand-field analysis.

With the relabeled data, then, reproduction of the ESR experiment was found to be most sensitive to the e_π and $e_{\pi\sigma}$ parameter values, with e_σ and *B* values determined more by the d–d transition energies. Despite

(1) Deeth, R. J.; Duer, M. J.; Gerloch, M. *Inorg. Chem.* **1987**, *26*, 2573.
(2) Deeth, R. J.; Duer, M. J.; Gerloch, M. *Inorg. Chem.* **1987**, *26*, 2578.
(3) Deeth, R. J.; Gerloch, M. *Inorg. Chem.* **1987**, *26*, 2582.
(4) Fenton, N. D.; Gerloch, M. *Inorg. Chem.* **1987**, *26*, 3273.
(5) (a) CAMMAG2, a FORTRAN computing package by A. R. Dale, M. J. Duer, M. Gerloch, and R. F. McMeeking. (b) Gerloch, M.; Woolley, R. G. *Prog. Inorg. Chem.* **1984**, *31*, 371. (c) Brown, C. A.; Gerloch, M.; McMeeking, R. F. *Mol. Phys.* **1988**, *64*, 771. (d) Gerloch, M. *Magnetism & Ligand-Field Analysis*; Cambridge University Press: Cambridge, England, 1983; p 305. (e) Gerloch, M.; McMeeking, R. F. *J. Chem. Soc., Dalton Trans.* **1975**, 2443.
(6) Bertini, I.; Dapporto, P.; Gatteschi, D.; Scozzafava, A. *Inorg. Chem.* **1975**, *14*, 1639.
(7) Bencini, A.; Benelli, C.; Gatteschi, D.; Zanchini, C. *Inorg. Chem.* **1980**, *19*, 3839.

0020-1669/89/1328-2767$01.50/0

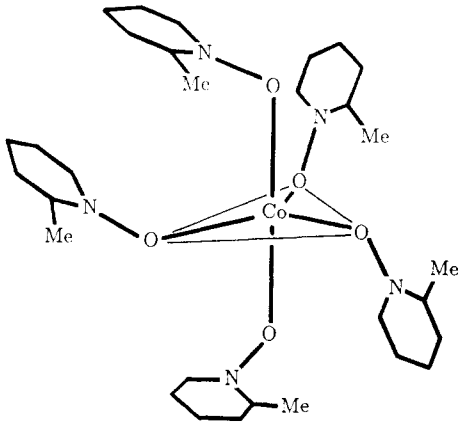

Figure 1. Coordination geometry in the pentakis(picoline *N*-oxide) cobalt(II) ion.

Table I. $[(\text{Picoline } N\text{-oxide})_5\text{Co}]^{2+}(\text{ClO}_4^-)_2$: Comparison between Observed[7] $\mathbf{g}^2$ Tensor and That Calculated with the Optimal Parameter Values of Table VII

obsd[a]				calcd			
principal g value	orientation (deg) ref to			principal g value	orientation (deg) ref to		
	a	b	c'		a	b	c'
1.86	14	81	80	1.89	12	79	84
3.53	98	103	15	3.54	93	106	17
5.67	79	164	101	5.67	78	160	105

[a] The $\mathbf{g}^2$ tensor in ref 7 was incorrectly labeled in this order by c', b, and a.

Table II. $[(\text{Picoline } N\text{-oxide})_5\text{Co}]^{2+}(\text{ClO}_4^-)_2$: Comparison between Observed[6] Transition Energies (cm^{-1}) for Spin-Allowed Bands with Those Calculated with the Optimal Parameter Values of Table VII

obsd	calcd	obsd	calcd
18 000	19 914	ca. 5000?	4970
	17 974		4272
	16 930		2206
12 500	12 647		1300
10 200	10 062		0

Table III. $[(\text{Picoline } N\text{-oxide})_5\text{Co}]^{2+}(\text{ClO}_4^-)_2$: $\mathbf{g}^2$ Tensor Calculated within the Spin-Quartet Basis by Using Parameter Sets of Ref 7

principal g value	orientation (deg) ref to		
	a	b	c'
1.90	15	75	89
3.59	93	84	7
5.87	75	163	83

the large number of variables, an essentially unique region of parameter space defined a simultaneous "best fit" to these optical and magnetic properties. That best fit was deficient, however, in that the magnitudes of the calculated principal g values differed from experiment by about 0.15. However, extension of the computational basis from spin quartets only to the full d^7 configuration yielded virtually perfect agreement with experiment following small changes in some parameter values. A nominal value only for C was used, good reproduction of all properties being achieved with the lowest calculated doublet lying anywhere between 12 000 and 15 000 cm^{-1}. Comparison between the observed $\mathbf{g}^2$ tensor and that calculated with the optimal parameter set is shown in Table I. Similar comparison of transition energies in the optical spectra are given in Table II. The best-fit parameter values are listed later in Table VII. Bencini et al.[7] report best reproduction of the $\mathbf{g}^2$ tensor with the following parameter set: $e_\sigma(\text{ax}) = 4725\ cm^{-1}$, $e_\pi(\text{ax}) = 1185\ cm^{-1}$, $e_\sigma(\text{eq}) = 5250\ cm^{-1}$, $e_\pi(\text{eq}) = 1315\ cm^{-1}$, $B = 850\ cm^{-1}$, $\zeta = 533\ cm^{-1}$, and $k = 0.85$. Their calculated (relabeled) $\mathbf{g}^2$ tensor is given in Table III and is characterized by fair magnitudes of the principal g values but an orientation some 20° different from that observed. Throughout our analysis we noted how this level of agreement with experiment is achievable for a very wide selection of parameter values in which the experimental orientation is only reproduced for the essentially unique parameter set reported in Table VII. Of particular concern is the value of the ligand-field trace, Σ (given by the sum of all diagonal e_λ parameter values), associated with Bencini et al.'s fit. At $\Sigma = 37\,850\ cm^{-1}$, we observe a value far larger than those usually observed[8] for this type of system, namely, 21 000–29 000 cm^{-1}.

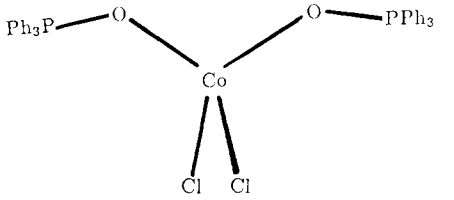

Figure 2. Coordination geometry in dichlorobis(triphenylphosphine)cobalt(II).

Table IV. $CoCl_2(OPPh_3)_2$: Comparison between Observed[11] $\mathbf{g}^2$ Tensor and That Calculated with the Optimal Parameter Values of Table VII

obsd[a]				calcd			
principal g value	orientation (deg) ref to			principal g value	orientation (deg) ref to		
	a	b	c		a	b	c
2.16	30	60	90	2.14	32	58	90
3.59	90	90	0	3.60	90	90	0
5.67	120	30	90	5.68	122	32	90

[a] From cobalt-doped zinc analogue[9] in which the molecular diad lies parallel to the crystal c axis.

Table V. $CoCl_2(OPPh_3)_2$: Comparison between Observed[11] Transition Energies (cm^{-1}) for the Spin-Allowed Bands with Those Calculated with the Optimal Parameter Values of Table VII

obsd	calcd	obsd	calcd
16 500	16 150		4706
15 000	15 360		3376
	14 923		3024
ca. 6800[a]	6762		2780
	5688		0

[a] Claimed in ref 11. The spectral trace also suggests the presence of further transitions at lower energies.

Table VI. $CoCl_2(OPPh_3)_2$: $\mathbf{g}^2$ Tensors Calculated within the Spin-Quartet Basis by Using Parameter Sets of Ref 11 for Two Definitions of $e_{\pi s}$[a]

$e_{\pi s} = e_{\pi\perp}$				$e_{\pi s} = e_{\pi\parallel}$			
principal g value	orientation[b] (deg) ref to			principal g value	orientation (deg) ref to		
	a	b	c		a	b	c
1.62	30	60	90	1.05	41	49	90
2.30	90	90	0	1.26	90	90	0
6.72	120	30	90	7.26	139	41	90

[a] See text. [b] Values quoted to nearest degree.

Dichlorobis(triphenylphosphine oxide)cobalt(II). The zinc analogue[9] of this complex, used as a host lattice for single-crystal ESR spectroscopy, differs structurally only slightly from the cobalt[10] system. A crystallographic diad in the zinc molecule is lost in the cobalt one following small displacements of the outer phenyl groups. Our ligand-field analysis considers just two ligand types—chlorine and phosphine oxide. The coordination geometry is shown in Figure 2. The CLF parameter sets comprise e_σ and e_π for the linearly ligating chlorines and e_σ, $e_{\pi\perp}$, $e_{\pi\parallel}$, and $e_{\pi\sigma}$ for the phosphine oxides. As for the five-coordinate molecule above, the parameter set includes B, C, ζ, and k variables.

Again, the spectra[11] are not rich. We can exploit the splitting of the ^4P term, the energy of, e.g., its baricenter, mainly to establish the B value,

(8) Deeth, R. J.; Gerloch, M. *J. Chem. Soc., Dalton Trans.* **1986**, 1531.
(9) Rose, J. P.; Lalancette, R. A.; Potenza, J. A.; Schugar, H. J. *Acta Crystallogr.*, **1980**, *B36*, 2409.
(10) Mangion, M. M.; Smith, R.; Shaw, S. G. *Cryst. Struct. Commun.* **1976**, *5*, 493.
(11) Bencini, A.; Benelli, C.; Gatteschi, D.; Zanchini, C. *Inorg. Chem.* **1979**, *18*, 2137.

Table VII. Optimal Parameter Values (cm^{-1}) Yielding Accurate Reproduction of Observed Ligand-Field Properties

$Co(OPPh_3)_2Cl_2$[a]		$[Co(OpyCH_3)_5](ClO_4)_2$[a]		$[Co(Opy)_6](ClO_4)_2$[b]	
$e_\sigma(O)$	3500 (100)[c]	$e_\sigma(eq)$	4550 (100)[c]	e_σ	3500
$e_{\pi\perp}(O)$	900 (50)	$e_{\pi\perp}(eq)$	400 (100)	$e_{\pi\perp}$	850
$e_{\pi\parallel}(O)$	600 (75)	$e_{\pi\parallel}(eq)$	1450 (75)	$e_{\pi\parallel}$	450
$e_{\pi\sigma}(O)$	−100 (50)	$e_{\pi\sigma}(eq)$	500 (25)	$e_{\pi\sigma}$	700
$e_\sigma(Cl)$	3350 (100)	$e_\sigma(ax)$	4150 (100)		
$e_\pi(Cl)$	800 (100)	$e_{\pi\perp}(ax)$	75 (25)		
		$e_{\pi\parallel}(ax)$	550 (75)		
		$e_{\pi\sigma}(ax)$	50 (50)		
Σ	19900	Σ	28750	Σ	28800
B	770 (25)	B	825 (25)	B	815
C[d]	2750	C[d]	3000	C[d]	3033
$k\zeta$	420 (30)	$k\zeta$	340 (30)	$k\zeta$	400

[a] This work. [b] From a reanalysis of an earlier study.[15] For $[Co(Opy)_6](ClO_4)_2$, correlations exist between parameter values: for example, with Σ chosen as 25 800 cm^{-1}, e_σ = 3400, $e_{\pi\perp}$ = 650, $e_{\pi\parallel}$ = 250, $e_{\pi\sigma}$ = 700, B = 815, C = 3033, and $k\zeta$ = 400 cm^{-1}. [c] Estimated errors in parentheses. [d] Fixed values.

and a window between ca. 7000 and 14 000 cm^{-1}. A weaker feature at 13 000 cm^{-1} can only be reproduced as of spin-forbidden character. So, as for the previous complex, the ligand-field analysis rests heavily upon the single-crystal $\mathbf{g}^2$ tensor determination.[11] In other respects also, the two analyses were rather similar, the optical spectrum fixing B and e_σ values in particular, the ESR experiment being reproduced mainly by the correct e_π and $e_{\pi\sigma}$ values. Once more, a unique fit was found and exact reproduction of the principal g values is ultimately possible only upon inclusion of the spin doublets into the computational basis. In the present case, k and ζ values are determined only as their product, $k\zeta$. Comparisons between the observed $\mathbf{g}^2$ tensor and that calculated with the optimal parameter set are shown in Table IV. Reproduction of transition energies is described in Table V. Optimal parameter values are listed in Table VII.

In Table VI are given molecular $\mathbf{g}^2$ tensors calculated with the previously published[11] angular overlap model (AOM) parameter set; $e_\sigma(Cl)$ = 5700 cm^{-1}, $e_\pi(Cl)$ = 2400 cm^{-1}, $e_\sigma(O)$ = 4750 cm^{-1}, $e_{\pi s}(O)$ = 1945 cm^{-1}, $e_{\pi c}(O)$ = 1555 cm^{-1}, B = 730 cm^{-1}, ζ = 533 cm^{-1}, and k = 0.9, for two definitions of local reference frames, depending on whether $e_{\pi s}$ is to be identified with the present $e_{\pi\parallel}$ or $e_{\pi\perp}$. It is clear that good reproduction of the optical and ESR data is not provided by the earlier scheme, though we note with curiosity that principal *crystal g* values calculated with these parameters (for $e_{\pi s} = e_{\pi\perp}$) are 2.30, 3.65, and 5.87, in fair agreement with the experimental *molecular* quantities. All these calculations were performed within the spin-quartet basis for easy comparison with the published computations. Enlarging the basis to the full d^7 configuration alters no g value by more than ca. 0.15. Again, the trace, Σ, of the parameter set above is very large, at 37 500 cm^{-1}.

Finally, that reproduction of the observed data is unsatisfactory when $e_{\pi\sigma}$ values are set to zero—that is, when the effects of misdirected valency are ignored—is illustrated in Appendix I.

Discussion

The combination of single-crystal electronic and high-quality ESR spectroscopy has provided a data base that has proved sufficient to define all the model parameters, essentially uniquely. The optimal parameter sets are given in Table VII.

Consider first the results for the five-coordinate picoline oxide complex. All e parameter values are smaller for the more distant axial ligands than for their equatorial counterparts. As might be expected, the π parameters are more sensitive to the bond length difference than are the σ ones. The patterns of values for $e_{\pi\perp}$, $e_{\pi\parallel}$, and $e_{\pi\sigma}$ are qualitatively similar. As all the angles ∠Co–O–N are close to 120°, we presume that a simple sp^2 hybridization on the donor oxygen atoms is a satisfactory description, so that the nonzero values of $e_{\pi\sigma}$ reflect the presence of the nonbonding lone pair rather than any bent bonding. The positive signs for these parameters accord with that proposal.[1] While the values for $e_{\pi\perp}$ indicate modest π-donor roles for the oxygen ligands in the planes perpendicular to the appropriate Co–O–N triads, those for $e_{\pi\parallel}$ again reflect the density of the oxygen sp^2 nonbonding lone pair. For both axial and equatorial picoline oxide ligands, the ligand-field contributions from these lone pairs to $e_{\pi\parallel}$ are larger than those from the p_π lone pairs oriented perpendicular to the Co–O–N triads. That $e_{\pi\parallel} > e_{\pi\perp}$ for these ligations is an important feature of this analysis and a matter to which we return shortly.

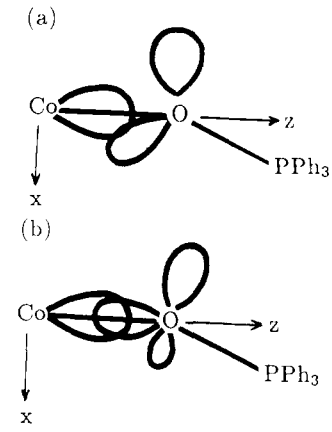

Figure 3. Two views of the Co–O bonding in dichlorobis(triphenylphosphine)cobalt(II): (a) with formal sp^2 hybridization of the donor oxygen atom, there results bent bonding and an sp^2 lone pair in the negative xz quadrant; (b) with hybridization between sp^2 and sp, the "nonbonding" lone pair of the oxygen atom possesses significant lobes in both negative and positive quadrants.

The Co–O bond lengths in the phosphine oxide complex are much the same as those for the equatorial sites in the picoline oxide molecule. On the other hand, the ligand-field strengths of these two groups as monitored by their e_σ values are markedly different. It is not altogether arbitrary to assert that the picoline *N*-oxide ligands are strong donors rather than that the phosphine oxides are weak. This remark is based on the values found[8] for the ligand-field trace, Σ, being the sum of all diagonal e_λ values in the complex. We have repeatedly demonstrated the near constancy of the trace with respect to variation of coordination number and geometry and, for many ligands, of ligand type, all for first-row metals in the +2 oxidation state. We suspect that the constancy of the trace reflects the operation of the electroneutrality principle but not apparently in a totally straightforward manner. Some variation in trace values has been observed, low values for complexes with phosphines, high values with imines. Larger variations are apparent within metal(III) species.[12] So, for the present complexes, the phosphine oxide system is characterized by a trace that fits what might be termed the "normal" pattern, while the large value of ca. 29 000 cm^{-1} for the picoline oxide complex does not.

Of especial interest in the phosphine oxide complex are the e_π and $e_{\pi\sigma}$ values. First, we observe a small and negative value for $e_{\pi\sigma}(O)$. As this is associated with a significant value for $e_{\pi\parallel}(O)$, we are not to conclude that the effects of misdirected valency are negligible. Instead, we interpret these e values in terms of the effects of a nonbonding lone pair combined with those of either a bent bond or a changed hybridization of the donor atom, as follows. The angle ∠Co–O–P is ca. 150°. If we view the cobalt–oxygen bond as strongly bent as a result of interaction of the metal with an oxygen sp^2 hybrid, we expect a large contribution to $e_{\pi\sigma}$, which, in view of its location in the positive local xz quadrant (Figure 3a), will be of negative sign.[1] The small, negative value for $e_{\pi\sigma}$ actually found by ligand-field analysis is then to be seen as the net effect from a bent bond with the positive contribution from the nonbonding sp^2 lone pair lying in the negative xz quadrant. The effects of both sources of misdirected valence upon $e_{\pi\parallel}(O)$, on the other hand, will be of positive sign, and so no similar concellation occurs. Alternatively, if we suppose the local Co–O σ bond to be well directed along the line of centers, we must adopt another description of the oxygen hybridization, namely, something between sp^2 and sp. In this case, the "nonbonding" lone pair gains more p character and might resonably be sketched as in Figure 3b. Here we interpret the observed small and negative value for

(12) Fenton, N. D.; Gerloch, M. *J. Chem. Soc., Dalton Trans.* **1988**, 2201.

$e_{\pi\sigma}$(O) as the net result of a larger, negative contribution from the more metal-directed lobe of the lone pair in the positive quadrant offset to some extent by a smaller, positive contribution from the less metal-directed lobe in the negative quadrant. Once again, the contributions from both lobes to $e_{\pi\parallel}$(O) will be arithmetrically additive.

Some comparison with the analogous dichlorobis(trimethylphosphine oxide)cobalt(II) complex is possible. While an unpolarized electronic absorption spectrum has been reported,[13] there has unfortunately been no detailed study of the ESR spectrum so that we are unable to undertake a useful ligand-field analysis. However, an X-ray structural analysis has been reported.[14] The significant difference between the two complexes is that the angle ∠Co–O–P for the trimethyl analogue is ca. 130° instead of 150° as for the triphenyl system. At the same time, the Co–O and O–P bond lengths in the two complexes are the same within experimental error, as are the various coordination angles about the phosphorus atom (essentially tetrahedral). These latter features, together with simple model building, suggest that the different Co–O–P angles are not the result of intramolecular packing constraints. Instead, we infer an electronic origin for the difference, reflecting the greater inductive drive of the methyl groups. These would increase the negative charge on the oxygen relative to that in the triphenyl ligand, so enlarging the bulk of the lone pairs, which, in turn, would encourage a less linear disposition of electron density around the oxygen atom. This line of argument links well with the phenomenon of $e_{\pi\parallel} > e_{\pi\perp}$ in the pentakis(picoline) complex described above and to which we now return.

That $e_{\pi\parallel} > e_{\pi\perp}$ for the picoline ligations appears to be unusual, at least by comparison with the phosphine oxide complex, with several other systems revealing the ligand-field effects of misdirected valency,[1-4] and generally with the idea that the lone pairs in such systems are expected to be oriented somewhat away from the metal. The analytical result is certain, nevertheless. It is interesting to compare it with the equally sure conclusions of an analysis[14] of the magnetic anisotropy of the complex hexakis(pyridine *N*-oxide)cobalt(II) diperchlorate. In that study, the sign of the magnetic anisotropy is the determinant of the sign of ($e_{\pi\parallel} - e_{\pi\perp}$) and is such that $e_{\pi\parallel} < e_{\pi\perp}$. No account of the effects of misdirected valency was taken in that early analysis, and so we have reinvestigated this system on the same basis as chosen for the present complexes. Unfortunately, the high molecular symmetry of the hexakis(pyridine oxide) complex renders the magnetic anisotropy and electronic absorption spectral data inadequate to support a unique ligand-field analysis. Excellent reproduction of the reported[15] susceptibilities is possible but within ranges of ligand-field parameter values. The ambiguity is characterized essentially by correlated "best-fit" values of $e_{\pi\parallel}$, $e_{\pi\perp}$, and $e_{\pi\sigma}$ as noted in Table VII. However, all reasonable choices—that is, with either $e_\pi < 2000$ cm^{-1}—are such that $e_{\pi\parallel} < e_{\pi\perp}$ in confirmation of the earlier analysis that did not include the $e_{\pi\sigma}$ variable. Within the ranges of possible fits, the minimum trace, Σ, is ca. 26 000 cm^{-1} so that a similar behavior for pyridine oxides as for picoline oxides appears likely. For purposes of illustration and comparison, we report in Table VII an optimal parameter set that is associated (uniquely) with the choice of $\Sigma = 29\,000$ cm^{-1}, as for the picoline system. Two features of that parameter set are qualitatively certain and important for our present purposes. First, despite the similar Co–O bond lengths (pyridine complex[15] and axial picoline), e_σ takes a value considerably smaller for the hexakis(pyridine oxide) complex than for the pentakis(picoline oxide) one. We suppose this to reflect the different coordination numbers in that the one monitors the interaction of pyridine *N*-oxide with a (pyridine *N*-oxide)$_5$Co moiety, while the other refers to picoline *N*-oxide with a (picoline *N*-oxide)$_4$Co moiety. The second feature, again, is that $e_{\pi\parallel} < e_{\pi\perp}$ for the pyridine ligation but $e_{\pi\parallel} > e_{\pi\perp}$ for the picoline one. In view of the repeated and unbroken success of recent studies using the CLF model with a large variety of transition-metal complexes, we are disinclined to dismiss this conflict as an artifact of the ligand-field procedure. In short, we believe the difference is real and requires explanation.

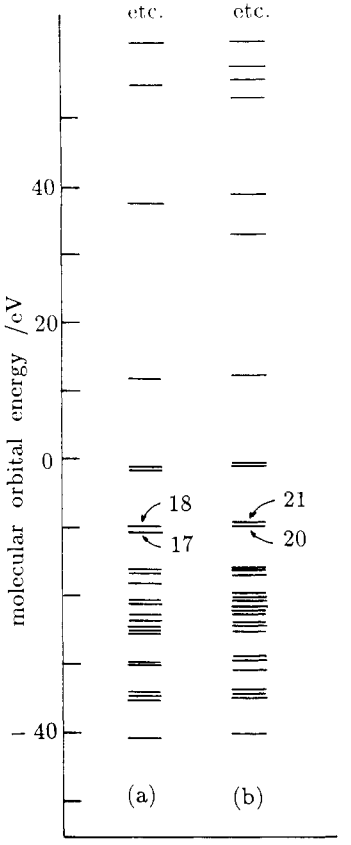

Figure 4. Molecular orbital energies from Fenske–Hall calculations for (a) pyridine *N*-oxide and (b) picoline *N*-oxide. The HOMO and sub-HOMO are labeled 18 and 17 for the pyridine *N*-oxide and 21 and 20 for the picoline *N*-oxide.

It is unlikely that we should find that explanation in terms of any differences between the ligands themselves. Nevertheless, we have undertaken Fenske–Hall, molecular orbital computations on both pyridine *N*-oxide and picoline *N*-oxide, details of which are presented in Appendix II. These confirm the very close similarity of the two molecules with respect to both energies and wave functions, especially for the near-degenerate HOMO and sub-HOMO orbitals. The calculations are interesting in another respect also. The HOMOs themselves leave ca. 95% O $2p_\perp$ character (that is, the p orbitals perpendicular to the planes of the molecules) and so are essentially pure $p_\perp$ atomic orbitals, as would be represented diagramatically by I. Only 1 eV deeper

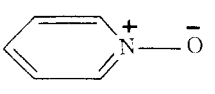

I

than the energy of the HOMO in each case lies a molecular orbital that is dominated by some 75% O $2p_\parallel$ character. That this orbital is less atomic than the HOMO arises from the interaction of the oxygen $p_\parallel$ atomic orbital with the bonding framework of the pyridine (picoline) group.

Now we observe that both picoline oxide and pyridine oxide ligations in our two complexes are such that the metal atom invariably lies out of the plane of the heterocycle rather than in that plane and displaced to one side as might have been envisaged if the oxygen atom is formally sp^2 hybridized with the aforementioned $p_\perp$ orbital left unhybridized. A common line of argument serves to rationalize this coordination geometry and the differing relative magnitudes of $e_\parallel$ and $e_{\pi\perp}$ determined for the two complexes by ligand-field analysis. In the free ligands, a view along the O–N axis toward the nitrogen atom would reveal a cone

(13) Cotton, F. A.; Barnes, R. D.; Bannister, E. *J. Chem. Soc.* **1960**, 2199.
(14) Edelmann, F.; Behrens, U. *Acta Crystallogr.* **1986**, *C42*, 1715.
(15) Mackey, D. J.; Evans, S. V.; McMeeking, R. F. *J. Chem. Soc., Dalton Trans.* **1978**, 160.

Table VIII. Valence Atomic Orbital Coefficients in HOMO and Sub-HOMO Molecular Orbitals of Pyridine *N*-Oxide and Picoline *N*-Oxide

atomic orbital	pyridine *N*-oxide		picoline *N*-oxide	
	HOMO	sub-HOMO	HOMO	subHOMO
O 2s	0.00	0.00	0.00	0.00
O $2p_\perp$	−1.00	0.00	−1.00	0.03
O $2p_\parallel$	0.00	0.86	0.03	0.87
O $2p_z$	0.00	0.00	0.00	0.01
N 2s	0.00	0.00	0.00	0.00
N $2p_\perp$	0.10	0.00	0.10	0.00
N $2p_\parallel$	0.00	0.04	0.00	0.02
N $2p_z$	0.00	0.00	0.00	0.00
C_2 2s	0.07	0.00	0.06	0.00
C_2 $2p_\perp$	−0.12	0.00	−0.11	0.00
C_2 $2p_\parallel$	0.00	−0.33	0.00	−0.32
C_2 $2p_z$	−0.08	0.00	−0.08	0.01
C_3 2s	−0.01	0.00	−0.01	0.00
C_3 $2p_\perp$	0.01	0.00	0.02	0.00
C_3 $2p_\parallel$	0.00	0.02	0.00	−0.02
C_3 $2p_z$	0.02	0.00	0.02	0.00
C_4 2s	0.00	0.00	0.00	0.00
C_4 $2p_\perp$	−0.03	0.00	−0.02	0.01
C_4 $2p_\parallel$	0.00	0.33	0.00	0.33
C_4 $2p_z$	0.00	0.00	0.00	0.01
C_5 2s	0.01	0.00	0.01	0.00
C_5 $2p_\perp$	0.02	0.00	0.02	0.00
C_5 $2p_\parallel$	0.00	0.02	0.00	0.05
C_5 $2p_z$	−0.02	0.00	−0.02	0.00
C_6 2s	−0.07	0.00	−0.06	0.00
C_6 $2p_\perp$	−0.12	0.00	−0.11	0.00
C_6 $2p_\parallel$	0.00	−0.33	0.00	−0.30
C_6 $2p_z$	0.09	0.00	0.07	0.01
C_7 2s			0.01	0.00
C_7 $2p_\perp$			0.01	0.00
C_7 $2p_\parallel$			0.01	0.04
C_7 $2p_z$			−0.01	0.00
H_2 1s	−0.01	0.00		
H_3 1s	0.04	0.00	0.04	0.00
H_4 1s	0.00	0.00	0.00	0.00
H_5 1s	−0.04	0.00	−0.03	0.00
H_6 1s	0.01	0.00	0.00	0.00
H_a 1s			0.00	−0.07
H_b 1s			0.01	0.00
H_c 1s			0.00	0.07
energy/eV	−9.3416	−10.2278	−8.8491	−9.5615

of "π" charge roughly of cylindrical symmetry extending out from the oxygen atoms. However, the inaccuracy of the circular symmetry would be such that more charge would appear in the plane perpendicular to the heterocycle than parallel to it. Attack by an electrophile in the form of the transition metal will then be expected to take place preferentially in the plane perpendicular to the heterocycle, as is indeed observed. In forming a (σ) bond with the metal, the bonding electrons will collapse about the line of centers (M–O) and so offer a decreased repulsion to the remaining nonbonding oxygen lone pairs. In turn, that lone-pair electron density will tend to move somewhat closer to the M–O bond-pair density. Seen as a continuous change from a distant or weak metal acceptor toward a close or strong one, the movement of the nonbonding oxygen lone pair toward the metal–oxygen vector is expected to increase with greater metal acceptor power. Recall now, the difference between the hexakis(pyridine *N*-oxide) and pentakis(picoline *N*-oxide) complexes. The much smaller e_σ value in the former case reflects the lesser acceptor role of (pyridine *N*-oxide)$_5$Co with respect to (picoline *N*-oxide)$_4$Co. We thus view the smaller value of $e_{\pi\parallel}$ in the pyridine *N*-oxide complex as a further reflection of the lesser acidity of the (pyridine *N*-oxide)$_5$Co moiety. That $e_{\pi\parallel}$ in the picoline *N*-oxide complex is greater follows by the converse, and that it is so large anyway is a reflection of the formal negative charge on the oxygen in the free ligand, as in I.

Conclusions

Unambiguous determinations of the cellular ligand fields in the four- and five-coordinate complexes have been possible by accurate reproductions of single-crystal electronic absorption and ESR spectroscopic data. The phosphine oxide and picoline *N*-oxide ligations are both characterized by locally nondiagonal ligand fields whose origins are explicable in detail in terms of mainstream chemical bonding vocabulary. A common feature between our understanding of the different Co–O–P angles in the triphenyl and trimethyl analogues on the one hand, and of the relative magnitudes of $e_{\pi\parallel}$ and $e_{\pi\perp}$ for the pentakis(picoline *N*-oxide) and hexakis(pyridine *N*-oxide) species, on the other, is a recognition of the various interelectron repulsions between bonding and nonbonding lone pairs as discussed so long ago by Gillespie and Nyholm.[16]

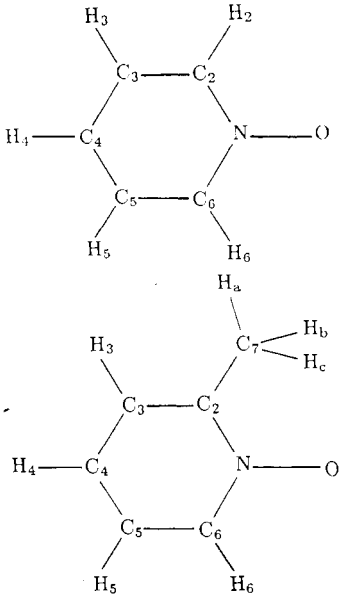

Figure 5. Atom labeling used for the Fenske–Hall calculations. Valence orbital coefficients in Table VIII refer to directions parallel (∥) and perpendicular (⊥) to the planes of the heterocycles and to *z* lying parallel to the N–O vectors.

Acknowledgment. We are most grateful to Dr. E. C. Constable for valuable discussions and to Dr. C. Housecroft and S. M. Owen for their introduction to the Fenske–Hall computer program. N.D.F. thanks the SERC for a research studentship.

Appendix I

We summarize here the results of some calculations that demonstrate the importance of the $e_{\pi\sigma}$ parameters in these analyses.

(a) $Co(OPPh_3)_2Cl_2$. The value of $e_{\pi\sigma}(O)$ quoted in Table VII is only −100 cm^{-1}. Here we consider the effects of setting $e_{\pi\sigma}(O)$ to 0. First, we observed that calculated eigenvalues shift by ca. 50 cm^{-1} at most, so providing no evidence for the nonzero value. However, calculated *g* values do change significantly. Instead of the magnitude and orientations given in Table IV, we now have the following:

principal *g* value	orientation (deg) ref to		
	a	*b*	*c*
2.08	29	61	90
3.36	90	90	0
5.83	119	29	90

We note that the calculated orientation of the $\mathbf{g}^2$ tensor changes little but that the values of the principal *g* values suffer markedly from the neglect of $e_{\pi\sigma}(O)$. The good agreement with experiment, shown in Table IV, is *not* restored with $e_{\pi\sigma}(O) = 0$ taken together with variations in other parameters.

(b) $[Co(OpyCH_3)_5](ClO_4)_2$. Similarly setting either or both $e_{\pi\sigma}$ values in Table VII to zero for this complex makes only marginal differences to calculated eigenvalues and hence transition energies. Once more, it is the sensitivity of the $\mathbf{g}^2$ tensors to $e_{\pi\sigma}(O)$ that

(16) Gillespie, R. J.; Nyholm, R. S. *Quart. Rev. Chem. Soc.* **1957**, *11*, 339.

establishes the nonzero values of these parameters. Instead of the good agreement with experiment shown in Table I, we obtain the following results with variation of the $e_{\pi\sigma}$(O):

(i) with $e_{\pi\sigma}$(ax) = 0 (other parameters as in Table VII)

principal g value	orientation (deg) ref to a	b	c'
1.89	12	79	84
3.50	93	109	19
5.72	79	157	108

(ii) with $e_{\pi\sigma}$(eq) = 0 (other parameters as in Table VII)

principal g value	orientation (deg) ref to a	b	c'
1.87	16	74	89
3.26	93	76	166
5.87	74	159	104

Variations in either $e_{\pi\sigma}$ value by these magnitudes, but in combination, give results essentially as might be guessed from these individual responses. Altogether, neglect of $e_{\pi\sigma}$(eq) is again not recompensed by variation of the remaining parameters. Many calculations of this nature have led to the error estimates in Table VII.

Appendix II

Fenske-Hall calculations[17] were carried out on both pyridine *N*-oxide and picoline *N*-oxide. Molecular geometries were taken from reported X-ray structural analysis[18,19] except for C-H distances in the pyridine oxide ligand, which were idealized to lie at 0.98 Å from appropriate carbon atoms. Basis functions were chosen as single Slater orbitals for the 1s and 2s functions of N, C, and O, in which exponents were obtained by curve-fitting the double-ζ functions of Clementi[20] but with retention of orthogonality. The 2p basis was represented by the double-ζ functions directly. For hydrogen, an exponent of 1.16 was used. Calculated molecular orbital energies are illustrated in Figure 4, from which the near identity of HOMOs and LUMOs in the two amine oxides is apparent. For each molecule, the HOMO and sub-HOMO are nearly degenerate. The characters of these two orbitals, in each system, are shown numerically in Table VIII with respect to valence atomic functions. The HOMOs are essentially pure atomic O $2p_{\perp}$ functions, and the sub-HOMOs are ca. 75% O $2p_{\parallel}$ with significant contributions from the framework of each heterocycle. Atom numbering is given in Figure 5, and $\parallel$ and $\perp$ relate to the planes of the heterocycles.

(17) Hall, M. B.; Fenske, R. F. *Inorg. Chem.* **1972**, *11*, 768.
(18) Ülkü, D.; Huddle, B. P.; Morrow, J. C. *Acta Crystallogr.* **1971**, *B27*, 432.
(19) Speakman, J. C.; Muir, K. W. *Croat. Chem. Acta* **1984**, *55*, 233.
(20) Clementi, E. *J. Chem. Phys.* **1964**, *40*, 1944.

Contribution from the Department of Chemistry,
The University of North Carolina at Chapel Hill, Chapel Hill, North Carolina 27599

Canted Antiferromagnetism in Single-Crystal Cobalt(II) Oxydiacetate Trihydrate

Brian R. Rohrs[1] and William E. Hatfield*

Received November 2, 1988

A single-crystal magnetic study of cobalt(II) oxydiacetate trihydrate is presented. The extended structure of $Co(C_4H_4O_5)\cdot 3H_2O$ consists of carboxylate-bridged cobalt(II) chains. The highly anisotropic principle magnetic susceptibilities display parallel and perpendicular Ising behavior in the b and a' directions. The susceptibilities are fit with the appropriate models where $J_{a'} = -8.84$ cm^{-1}, $g_{a'} = 2.193$ and $J_b = -6.44$ cm^{-1}, $g_b = 6.888$. A small xy contribution leads to a larger exchange coupling constant in the perpendicular (a') direction. Canting of the antiferromagnetically coupled moments along the cobalt chain (b) direction leads to weak ferromagnetism in the c' direction, and the various canting mechanisms are discussed in relation to $Co(C_4H_4O_5)\cdot 3H_2O$. The canting angle and interchain coupling are estimated from the magnetization and the critical field to be $\phi \approx 8.7°$ and $J_{c'} \approx -0.028$ cm^{-1}.

Previous work in our laboratory has shown that the layered compound copper(II) oxydiacetate hemihydrate[2] is an insulating ferromagnet. Since there are few molecular based, chelated coordination compounds that exhibit cooperative ferromagnetic behavior, the synthesis and characterization of other transition-metal oxydiacetate salts were undertaken. One of these, cobalt(II) oxydiacetate trihydrate, also exhibits cooperative magnetic behavior.[3] $Co(ODA)\cdot 3H_2O$ has the molecular structure shown in Figure 1. The coordination about the Co(II) ion consists of three oxygens from the tridentate oxydiacetate ligand (O1, O3, O5), two water molecules (OW1, OW2), and an oxygen from an adjacent oxydiacetate ligand (O2'). The distortion from an octahedral coordination geometry is significant. The ligand is nonplanar with the dihedral angle between the planes formed by O1-Co-O3 and O3-Co-O5 being 49.5°. A complete description of the crystal structure may be found in ref 3.

The linkage of the Co(II) ions to adjacent molecules via O2' leads to carboxylate-bridged cobalt chains that lie along the b direction. The chains, in turn, are bound together through weak hydrogen bonding to form sheets. From these structural considerations, one may expect primarily one-dimensional behavior with a small degree of higher dimensionality in the physical properties.[4] The powder magnetic susceptibility exhibits a sharp maximum below 3 K. The position of this peak is field dependent with an increase in the applied magnetic field leading to a decrease in $T(\chi_{max})$. This behavior is indicative of canted antiferromagnetism[5] and arises when the components of the moment vectors are not colinear. Measurements on single crystals were undertaken to determine the nature of the cooperative behavior.

Experimental Section

Synthesis. Cobalt(II) chloride (0.0025 mol) was dissolved in 200 mL of distilled water and oxydiacetic acid (0.0025 mol) was added with stirring. The solution was titrated with concentrated KOH solution until the cobalt solution turned cloudy (formation of $Co(OH)_2$). The solution was then back-titrated with 10 M HCl until the solution was clear again, and ~1 mL of excess 10 M HCl was added. This treatment removes the acidic protons on the oxydiacetic acid but keeps the solution acidic enough so that $Co(OH)_2$ does not form when the solution is concentrated. The solution was filtered and the filtrate then concentrated slowly by

(1) Current address: The Upjohn Company, Kalamazoo, MI 49001.
(2) Corvan, P. J.; Estes, W. E.; Weller, R. R.; Hatfield, W. E. *Inorg. Chem.* **1980**, *19*, 1297.
(3) Hatfield, W. E.; Helms, J. H.; Rohrs, B. R.; Singh, P.; Wasson, J. R.; Weller, R. R. *Proc.—Indian Acad. Sci., Chem. Sci.* **1987**, *98*, 23.
(4) See, for example: Groenendijk, H. A.; Van Duyneveldt, A. J. *Physica* **1982**, *115B*, 41.
(5) Silvera, I. F.; Thornley, J. H. M.; Tinkham, M. *Phys. Rev. A* **1964**, *136*, 695.

0020-1669/89/1328-2772$01.50/0